BIOCHEMISTRY

 Volume 47, Number 51 December 23, 2008

Articles

NMR Investigation of the Binding between Human Profilin I and Inositol 1,4,5-Triphosphate, the Soluble Headgroup of Phosphatidylinositol 4,5-Bisphosphate†

Sarah M. Richer,‡ Nichole K. Stewart,‡ John W. Tomaszewski,‡ Martin J. Stone,§ and Martha G. Oakley*,‡

Department of Chemistry, Indiana University, 800 East Kirkwood Avenue, Bloomington, Indiana 47405, and Department of Biochemistry and Molecular Biology, Monash University, Wellington Road, Clayton, Victoria 3800, Australia

Received August 13, 2008; Revised Manuscript Received October 20, 2008

ABSTRACT: Phosphatidylinositol 4,5-bisphosphate ($PI(4,5)P_2$) is involved in the regulation of the actin cytoskeleton through interactions with a number of actin-binding proteins. We present here NMR titration experiments that monitor the interaction between the cytoskeletal protein profilin and inositol 1,4,5-triphosphate (IP_3), the headgroup of $PI(4,5)P_2$. These experiments probe the interaction directly, at equilibrium, and with profilin in its native state. We show the binding between profilin and IP_3 can readily be observed at high concentrations, even though profilin does not bind to IP_3 under physiological conditions. Moreover, the titration data using wild-type profilin and an R88L mutant support the existence of at least three headgroup binding sites on profilin, consistent with previous experimentation with intact $PI(4,5)P_2$. This work suggests that various soluble inositol ligands can serve as effective probes to facilitate *in vitro* studies of PI-binding proteins that require membrane surfaces for high-affinity binding.

Phosphoinositide (PI)[1] lipids are key players in numerous processes in eukaryotic cells (*1*). Phosphatidylinositol 4,5-bisphosphate ($PI(4,5)P_2$) is the most abundant of the doubly phosphorylated PIs and has an effective cellular concentration of approximately 10 μM in typical mammalian cells (*2, 3*). This lipid is involved in a variety of cellular functions including membrane trafficking, activation of ion channels, GTPase signaling, and cellular growth and motility (*1, 4*−*9*). $PI(4,5)P_2$ interacts with a variety of structurally distinct binding domains including the PH, FERM, and ENTH domains. In addition, this lipid binds to a group of proteins that lack a specific binding domain but contain surface patches of basic residues (*2, 5, 10*−*17*). This lipid directly modulates the functions of numerous proteins, including profilin, WASP, and AP-2 (*1*).

Profilin I is a cytoskeletal protein that is found widely throughout eukaryotes and is essential in all organisms in which it has been studied (*18*). This small (15 kDa) globular protein binds three types of ligands: actin, PIP_2/PIP_3, and proteins that contain poly(L-proline) (PLP) stretches, including members of

† This work was supported by National Science Foundation Grant MCB-9722264 to M.G.O., National Institutes of Health Grant GM-55055 to M.J.S., and a Faculty Research Support Program award from the Office of the Vice Provost for Research at Indiana University to M.G.O. S.M.R. and N.K.S. were supported by GAANN fellowships from the Department of Education.

* Corresponding author. E-mail: oakley@indiana.edu. Tel: 812-855-4843. Fax: 812-855-08300.

‡ Indiana University.

§ Monash University.

[1] Abbreviations: $PI(4,5)P_2$, phosphatidylinositol 4,5-bisphosphate; IP_3, inositol 1,4,5-triphosphate; PI, phosphoinositide; PLP, poly(L-proline); PLC, phospholipase C; DAG, diacylglycerol; LB, Luria−Bertani; βMe, β-mercaptoethanol; K_d, dissociation constant.

10.1021/bi801535f CCC: $40.75
Published on Web 11/26/2008

the Ena/VASP, formin, and WASP/WAVE families (*19, 20*). Profilin functions in both the Arp2/3 and formin-dependent actin nucleation pathways and is thought to be required for proper cell migration and division (*19, 21*−*23*). Its actin-binding activity is associated with its ability to serve as a tumor suppressor in breast cancer lines (*24*−*28*). In addition, the PLP-binding activity of profilin appears to be important in cytoskeletal remodeling, vesicle trafficking, and nuclear profilin function (*19*). The actin- and PLP-binding regions of profilin are distinct from one another (*29, 30*). In contrast, $PI(4,5)P_2$ binding opposes binding of both actin and PLP, thereby providing a means for regulation of profilin by signal transduction pathways (*18, 31*−*34*).

Multiple regions of profilin have been implicated for $PI(4,5)P_2$ binding. Sohn et al. initially demonstrated the importance of Arg 88 by showing that mutation of this residue decreased profilin's ability to inhibit cleavage of $PI(4,5)P_2$ by phospholipase C (PLC) (*35*). Shortly thereafter, the N- and C-terminal helices were implicated as a binding site when Chaudhary et al. detected a covalent cross-link between Ala 1 of profilin and a PI photoaffinity tag (*36*). Molecular modeling suggested that Arg 135 and Arg 136, on the C-terminal helix, were the most probable residues for interaction with the PI headgroup (*36*). Later mutational studies using more direct binding methods supported a role for these two regions in $PI(4,5)P_2$ binding (*33, 34*). More recently, Lys 69 and Lys 90 have also been implicated by mutational analysis (*34*). However, single mutations generally have a modest impact on $PI(4,5)P_2$ binding, and these effects are highly dependent on the residue used for the particular point mutation (*33*). Moreover, the effects of these mutations have often been investigated indirectly, and none of the previous measurements has been made under equilibrium conditions (*26, 33*−*36*).

Although three-dimensional structures have been reported for the profilin·actin and profilin·PLP complexes, no structures have been reported for the profilin·$PI(4,5)P_2$ complex (*29, 37*). To our knowledge, only one crystal structure, solved recently, is available for any protein bound to an intact PI ligand (*38*). Moreover, the complex between $PI(4,5)P_2$ micelles and profilin, with an estimated molecular mass of approximately 270 kDa, is too large for high-resolution NMR analysis (*39*). In general, protein PI-binding sites have been structurally characterized by the use of soluble phosphoinositides such as inositol 1,4,5-triphosphate (IP_3), the headgroup of $PI(4,5)P_2$ (*40, 41*). However, no detectable binding has been observed between profilin and IP_3 (*20, 36, 42, 43*).

Nonetheless, several lines of evidence suggest that profilin interacts largely if not exclusively with the charged headgroup moiety of $PI(4,5)P_2$. Profilin is a soluble protein that associates with membranes in a peripheral manner, and its binding to $PI(4,5)P_2$ micelles results in no gross disruption of the micelle structure (*42, 44*). In addition, profilin can be dissociated from $PI(4,5)P_2$-containing membranes or vesicles through the use of a high salt buffer, suggesting that Coulombic interactions are the major driving force for the binding event (*45*). Finally, we have shown that covalent $PI(4,5)P_2$ micelle mimics completely lacking the diacylglycerol (DAG) chain can bind profilin with high affinity (S. M. Richer, N. K. Stewart, S. A. Webb, J. W. Tomaszewski, and M. G. Oakley, submitted for publication).

In spite of these considerations, profilin discriminates between $PI(4,5)P_2$ and IP_3 under physiological conditions, and this discrimination appears to be important for its biological function (*46*). One explanation for this phenomenon is that profilin is able to recognize higher local concentrations of $PI(4,5)P_2$ for interaction in a multivalent fashion. Supporting this view, profilin binds $PI(4,5)P_2$ with a measured stoichiometry of one molecule of profilin interacting with approximately five molecules of $PI(4,5)P_2$ (*39, 42*). Moreover, there appear to be regions within the plasma membrane that contain a higher local concentration of $PI(4,5)P_2$ (*47*). Finally, profilin binds to $PI(4,5)P_2$ at submicellar concentrations with a drastically reduced affinity compared to $PI(4,5)P_2$ micelles (*48*).

If profilin recognizes a multivalent display of $PI(4,5)P_2$ molecules through interaction primarily with the polar PI headgroup, then it should bind to IP_3, albeit with significantly reduced affinity. Moreover, the interaction of IP_3 will closely mimic that of $PI(4,5)P_2$, providing valuable information about the profilin·$PI(4,5)P_2$ complex. The investigation described herein utilizes NMR analysis to provide direct information concerning the binding of $PI(4,5)P_2$ to profilin under equilibrium conditions. We demonstrate that profilin does indeed bind IP_3, and we measure the affinity of this interaction. These results provide valuable information about the profilin·$PI(4,5)P_2$ interaction. Moreover, this work suggests that IP_3 is a useful tool not only for proteins that bind with high affinity to soluble PIs, but also for the study of peripheral membrane proteins that can discriminate *in vivo* between intact PIs and their hydrolysis products.

MATERIALS AND METHODS

Protein Expression and Purification. The plasmid encoding human profilin I (pMW172) was a kind gift from S. C. Almo. The Arg 88 to Leu mutation (R88L) was introduced using QuikChange site-directed mutagenesis (Stratagene). The DNA primers used for this point mutation were 5′-GAATTTAGCATGGATCTTCTGACCAAGAGCACCGGT-3′ and 5′-ACCGGTGCTCTTGGTCAGAAGATCCATGCTAAATTC-3′ (R → L mutation underlined). DNA sequencing was used to verify this mutation. Proteins were expressed using the T7 system in *Escherichia coli* BL21(DE3) cells (Novagen) (*49*). Unlabeled proteins were expressed in Luria−Bertani (LB) medium with 10 μg/mL ampicillin. Uniformly ^{15}N-labeled proteins were expressed in M9 minimal medium enriched with $^{15}NH_4Cl$ (Sigma-Aldrich) and supplemented with 10 μg/mL ampicillin. Purification and expression were achieved as described previously without the use of anion-exchange chromatography (*50, 51*). Additionally, we found that substitution of β-mercaptoethanol (βME) for dithiothreitol minimized protein precipitation and methionine oxidation. Therefore, 1 mM βME was used in all buffers. The proteins were concentrated using 3000 Da cutoff Amicon centrifugal filter devices (Millipore) and dialyzed into buffer A (20 mM Bis-Tris, 40 mM KCl, 20 mM βME, 10% D_2O, pH 6.4) for NMR experiments. Concentrations were determined utilizing Trp absorbance at 280 nm in 5−6 M guanidine hydrochloride (*52*). The masses of the purified proteins were confirmed by MALDI-TOF.

NMR Measurements and Resonance Assignments. All NMR spectra were collected at 20 °C on a Varian INOVA 500 MHz NMR spectrometer except for the three-dimensional TOCSY-HSQC and NOESY-HSQC experiments, which were performed at 20 °C on a Varian DirectDrive 600 MHz NMR spectrometer utilizing an HCN cold probe. Spectra were referenced to an external 2,2-dimethyl-2-silapentane-5-sulfonate (0 ppm) standard. The data were processed using VNMR (Varian) and viewed using Sparky version 3.111 (T. D. Goddard and D. G. Kneller, Sparky 3, University of California, San Francisco, CA) or processed and viewed using Felix98 (Molecular Simulations Inc., San Diego, CA). $^1H-^{15}N$ amide HSQC protein resonance assignments for human profilin I have been reported previously (*53*). Assignments for the R88L mutant were made primarily by comparison to the reported wild-type profilin HSQC assignments (*53*). All assignments were confirmed using three-dimensional TOCSY-HSQC and NOESY-HSQC experiments utilizing mixing times of 70 and 100 ms, respectively.

To investigate structural similarities between the mutant and wild-type proteins, the $^1H-^{15}N$ HSQC spectra of profilin and the R88L mutant were directly compared in the absence of IP_3. Peaks of the R88L mutant were considered to have no significant difference from those seen with the wild-type profilin if the ^{15}N resonances were within the error limits of 0.5 and 0.05 ppm for NH resonances according to the method described by Czerwinski et al. (*54*). Assignments were confirmed utilizing three-dimensional TOCSY-HSQC and NOESY-HSQC, as described above.

Observation of Binding between Profilin and IP_3 or Phosphate. To monitor binding between IP_3 and wild-type profilin, IP_3 was added stepwise in 6 μL increments to ^{15}N-labeled profilin at an initial concentration of 440 μM so that final stoichiometric ratios of IP_3 to profilin were 0, 0.82, 4.08, 8.17, 15, 20, 25, 30, 38, and 45. At each titration point the HSQC spectrum was recorded. The chemical shifts for individual profilin residues that change upon IP_3 binding were fit with Kaleidagraph (Synergy Software) to yield an apparent dissociation constant (K_d) using a 1:1 binding stoichiometry for species in fast exchange as described by Ye et al. (*55*). Only resonances with measurable shifts and goodness of fit parameters (R value) $\geq$ 0.995 were included.

To monitor binding between IP_3 and R88L profilin, a similar set of titration experiments was performed using an initial concentration of 421 μM ^{15}N-labeled R88L profilin and adding IP_3 in 6 μL increments. The final stoichiometric ratios of IP_3 to profilin were 0, 0.82, 4.08, 8.17, 15, 20, 25, 30, 38, and 45. The chemical shifts for the binding of IP_3 to the R88L profilin mutant were fit as above.

Titration of wild-type profilin with phosphate was performed with an initial profilin concentration of 349 μM and the addition of phosphate in 10 μL increments so that final stoichiometric ratios of phosphate to profilin were 0, 0.6, 1.2, 3.0, 6.0, 15, 24, 33, 45, 54, and 100.

In all titration series, the pH was carefully controlled and held within the range of 6.5 $\pm$ 0.1. To determine spectral changes at slightly elevated pH from the initial 6.4, a profilin HSQC spectrum was obtained at pH 6.8. Only two peak shifts were seen in this spectrum when compared to profilin at pH 6.4 (data not shown). These shifts were in the opposite directions in both ^{15}N and ^1H dimensions compared to those seen upon binding to IP_3. Thus, all peak shifts could be attributed to binding events.

RESULTS

Titration of Profilin I with IP_3. HSQC spectra of ^{15}N-labeled profilin were recorded in the absence and presence of increasing concentrations of IP_3. The IP_3 titrations resulted in concentration-dependent shifts of 30 resonances corresponding to backbone amides located primarily on one face of profilin (Figures 1 and 2, Table 1). The number of resonances that shift upon IP_3 binding is greater than is the case for PLP binding, suggesting a broader binding interface (*37*). Weighted chemical shift changes of profilin's amide backbone can be seen in Figure 1B. The residues that are affected by IP_3 are concentrated around site R88 and to a lesser extent R135/R136 and K69/K90 (Figure 2), consistent with previous mutational studies for profilin binding to $PI(4,5)P_2$ (*26, 33−36*). The IP_3 binding surface also overlaps with both the PLP- and actin-binding sites, consistent with the observation that $PI(4,5)P_2$ binding opposes binding of both of these ligands (*29, 37*). Thus, as expected, the binding of IP_3 to profilin closely mimics that of $PI(4,5)P_2$.

To determine a dissociation constant for the interaction between profilin and IP_3, the data for each shifting resonance were fit assuming a 1:1 binding model (Figure 1C, Table 1). The large number of residues affected by IP_3 binding strongly suggests binding by more than 1 equiv of this ligand. However, we could not distinguish isolated binding subsites for individual IP_3 molecules on the surface of profilin; indeed, we cannot rule out the possibility that changes in chemical shift for some amide resonances are affected by binding at more than one subsite. We therefore determined an average K_d for all sites of 19 $\pm$ 13 mM. As expected, this is significantly higher than the reported range of apparent K_d values (0.13−35 μM) for profilin's binding to $PI(4,5)P_2$ (*20, 33, 35, 45*).

The importance of Coulombic interactions in profilin's affinity for IP_3 was also investigated by an HSQC titration series with phosphate. Although concentration-dependent shifts were observed for several amide resonances at high phosphate concentrations, the affinity of profilin for IP_3 is clearly significantly higher than for phosphate, even when compared on a per phosphate basis (Figure 3). Indeed, the K_d value for the profilin·phosphate interaction is too high for reliable determination by NMR. Thus, the binding seen with IP_3 is specific and not merely a function of the nonspecific Coulombic interactions between the basic binding surface of profilin and a highly negatively charged ligand.

Titration of R88L Profilin with IP_3. In hopes of distinguishing the $PI(4,5)P_2$ binding subsites on profilin, we monitored the binding of IP_3 to a profilin mutant with approximately a 3-fold decrease in affinity for $PI(4,5)P_2$ (*35*). In the absence of IP_3, the $^1H-^{15}N$ HSQC spectra for the wild-type protein and for the R88L mutant are nearly superimposable, demonstrating that the three-dimensional structure of the protein is not significantly affected by the mutation. Indeed, 94% of ^{15}N resonances and 90% of ^1H_N resonances in the $^1H-^{15}N$ HSQC for R88L profilin are unaltered compared to the spectrum for wild-type profilin (data not shown) (*54*). As would be expected, the peaks that are shifted relative to the wild-type spectrum correspond to residues that are largely confined to the region of the mutation. In addition,

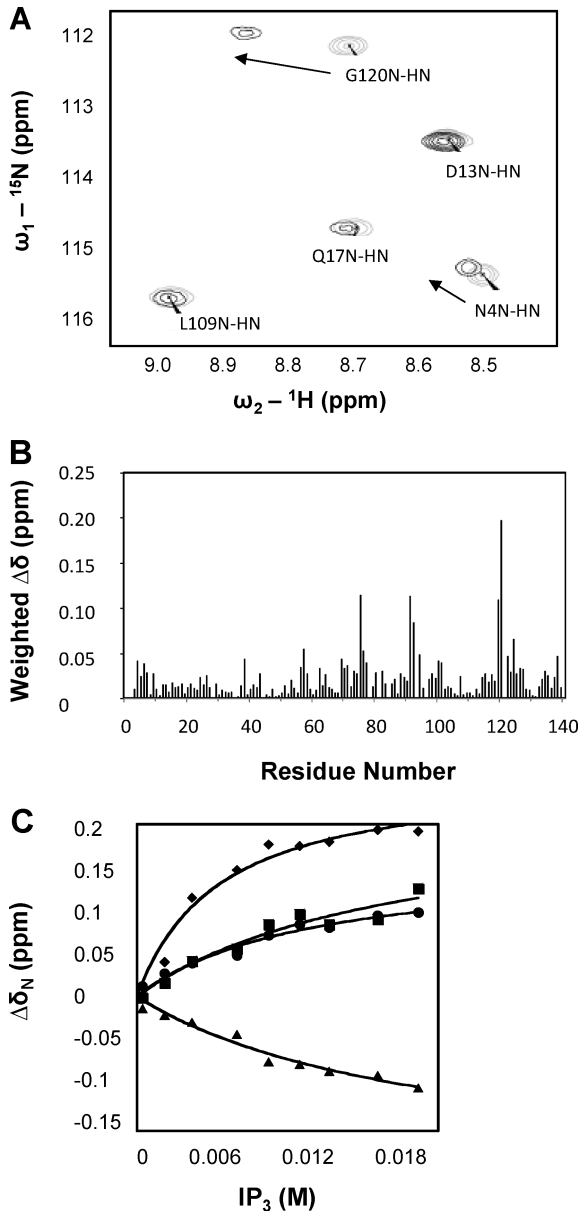

FIGURE 1: NMR detection of IP_3 binding to profilin. (A) A region of the $^1H-^{15}N$ HSQC spectra illustrating examples of changes in cross-peak chemical shifts as a result of profilin's interaction with IP_3. The overlaid spectra show profilin in the presence of IP_3 (IP_3/profilin = 45, black) and the absence of this ligand (gray). The profilin concentration was initially ~440 μM and decreased by approximately 10% throughout the titration. (B) Plot of weighted chemical shift ($\Delta\delta_{weighted} = |\Delta\delta_{^1H}| + 0.2|\Delta\delta_{^{15}N}|$) against the corresponding residue number. Weighted shifts were used to normalize shifts in both the ^1H and ^{15}N dimensions. As observed previously, solvent exchange or the absence of an amide proton resulted in the lack of chemical shift information for 13 residues (*53*). (C) Examples of binding curves used in dissociation constant determination. The amide nitrogen chemical shifts of Thr 64 (●), Asp 80 (■), Gly 120 (◆), and Ile 123 (▲) are plotted versus the IP_3 concentration. The curve fits allowed for a calculation of an average K_d of 19 mM.

the circular dichroism spectra of wild-type profilin and the R88L mutant are nearly identical (data not shown), also suggesting an unchanged global conformation.

In contrast, the $^1H-^{15}N$ HSQC spectra in the presence of IP_3 are significantly altered for the R88L protein relative to wild-type profilin. The number of peaks that exhibit concentration-dependent changes in chemical shift with increasing IP_3 concentration are substantially reduced, from 30 to 8, strongly supporting the importance of R88 in $PI(4,5)P_2$ and IP_3 binding. As expected, none of the residues in the vicinity of the R88L mutation site exhibited chemical shift changes. In addition, resonances corresponding to the N-terminal side of helix D, which is proximal to R88, are no longer affected by the presence of IP_3, suggesting a role for this helix in IP_3 and $PI(4,5)P_2$ binding (Figure 4, Table 2) (*56*). Finally, peaks corresponding to the C-terminal side of β-strand D and the turn that connects strands D and E, which are more distal to the mutation site, also fail to shift in the R88L mutant in the presence of IP_3 (Figure 4, Table 2) (*56*). The source of this change is not obvious.

The resonances corresponding to residues in the vicinity of the proposed K69/K90 and R135/R136 sites do show concentration-dependent shifts in the presence of IP_3 for the R88L mutant (*34, 36*). These data clearly demonstrate that IP_3 binding can occur at these sites even in the absence of R88. The apparent affinity of residues near site K69/K90 for IP_3 is unchanged in the mutant protein, with a K_d of 18 $\pm$ 4.4 mM. A small decrease in affinity is observed for the residues near site R135/R136, for which the measured average K_d is 44 $\pm$ 19 mM. This change may reflect an energetic coupling, possibly through helix D, between R135/R136 and the mutation site.

DISCUSSION

Using NMR titrations, we have established for the first time that profilin interacts specifically with IP_3, the headgroup of its target lipid $PI(4,5)P_2$. The chemical shifts of 30 residues are perturbed in a concentration-dependent manner by IP_3 binding, and the average apparent K_d of profilin for IP_3, as measured for these shifting peaks, is 19 $\pm$ 13 mM. As expected, this affinity is significantly lower than the values reported for the complex between profilin and $PI(4,5)P_2$ micelles or vesicles, with measured apparent K_d values ranging from 0.13 to 35 μM (*20, 33, 35, 45*). A similar difference in binding affinity has been demonstrated for mono- and multivalent carbohydrate probes toward proteins with multiple binding sites, suggesting the self-associated $PI(4,5)P_2$ molecules in membranes or micelles behave as a multivalent ligand for profilin (*57*−*59*). Indeed, the affinity of profilin for $PI(4,5)P_2$ at submicellar concentrations is substantially lower (K_d ~1 mM) than that seen with micelles or vesicles (*48*). The affinity of profilin for IP_3 is roughly 20-fold lower than that observed with submicellar concentration of $PI(4,5)P_2$. This observation may suggest that the intact lipid molecules self-associate on the surface of profilin through their hydrophobic tails, providing additional stability to the multivalent complex. Consistent with this interpretation, profilin clusters $PI(4,5)P_2$ in model membrane systems (*48*).

Although profilin binds IP_3 with reduced affinity relative to $PI(4,5)P_2$, the sites of interaction are consistent with the biochemical data for profilin's interaction with $PI(4,5P)_2$ (*26, 33*−*36*). Indeed, perturbed amide resonances were observed for residues at and adjacent to each of these three sites (Figure 2, Table 1). This observation suggests that IP_3 is an appropriate model for probing the binding interactions of $PI(4,5)P_2$, even for proteins that do not bind IP_3 under physiological conditions (*20, 36, 42, 43*).

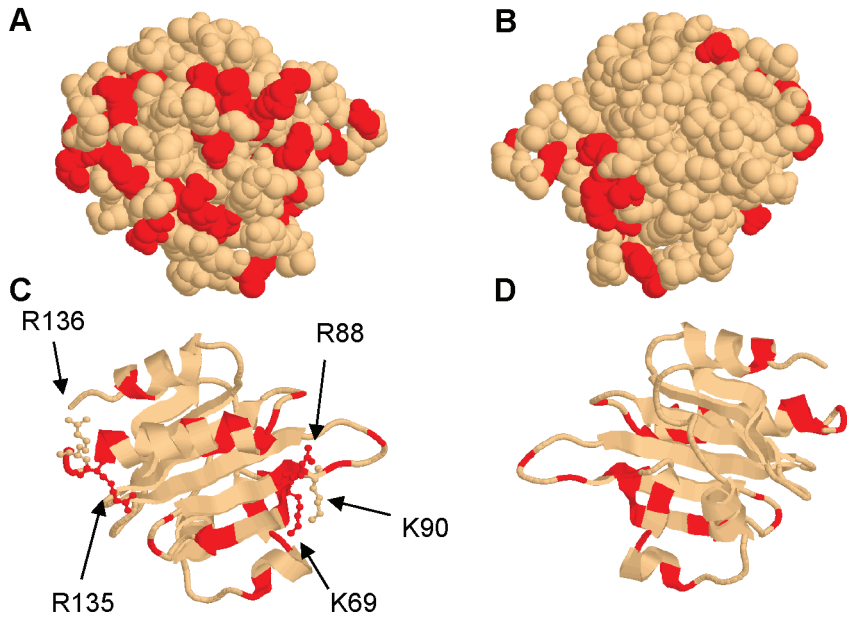

FIGURE 2: Structural mapping of profilin residues affected by IP_3 binding. Highlighted in red are the residues for which a chemical shift change was observed upon IP_3 binding. Shown in ball and stick representation are residues K69/K90, R88, and R135/R136. Structures in panels A and C show the positions of shifting residues on the face of wild-type profilin that includes the previously identified PI(4,5)P_2 binding sites. Structures in panels B and D show the opposite face of this protein. As expected, binding is seen primarily on one face of the protein. Residues affected by IP_3 on the opposite face of the protein are located primarily in loop regions or on the edges of the protein.

Table 1: Calculated K_d and $\Delta\delta_{max}$ Values for Each Shifting Residue in Wild-Type Profilin and the Error Associated with Each Value

residue	K_d (mM)	K_d error (mM)	$\Delta\delta_{max}$ (ppm)
N4 ^{15}N	13.8	3.2	0.180
Y6 ^{15}N	35.8	28.0	−0.370
S56 ^{15}N	16.8	5.5	0.224
S57 ^{15}N	37.5	16.0	−0.657
G62 ^{15}N	18.8	3.7	0.190
T64 ^{15}N	9.9	2.7	0.158
Q68 ^{15}N	7.8	3.6	−0.029
K69 ^{15}N	20.8	8.3	−0.280
C70 ^{15}N	14.1	4.5	−0.250
S71 ^{15}N	21.7	7.7	0.214
D75 ^{15}N	10.5	2.9	0.710
S76 ^{1}H	51.7	66.2	−0.192
D80 ^{15}N	15.1	7.4	0.220
E82 ^{15}N	32.1	16.1	0.193
R88 ^{15}N	16.9	1.8	0.194
T89 ^{15}N	57.5	29.4	0.348
S91 ^{15}N	26.0	6.9	−0.620
S91 ^{1}H	21.8	10.7	−0.151
G94 ^{15}N	15.4	4.6	0.260
G117 ^{15}N	14.1	5.7	−0.130
H119 ^{15}N	6.8	1.2	0.600
H119 ^{1}H	10.0	3.4	−0.041
G120 ^{15}N	4.6	1.1	0.260
G120 ^{1}H	11.9	3.0	−0.271
L122 ^{15}N	7.9	1.7	0.264
I123 ^{15}N	17.1	6.6	−0.210
N124 ^{1}H	16.7	7.1	−0.096
K126 ^{15}N	9.0	2.3	−0.168
H133 ^{15}N	1.5	0.8	0.088
L134 ^{15}N	14.7	5.0	0.127
R135 ^{15}N	17.7	8.0	0.097
S137 ^{15}N	22.4	10.3	−0.101
Q138 ^{15}N	28.6	16.7	−0.388

Perturbed amide resonances corresponding to residues that cover an entire face of profilin were observed in response to IP_3 binding. Thus, it is highly unlikely that these widespread shifts are caused by a single IP_3 molecule. However, on the basis of the wild-type titration alone, we could not rule out

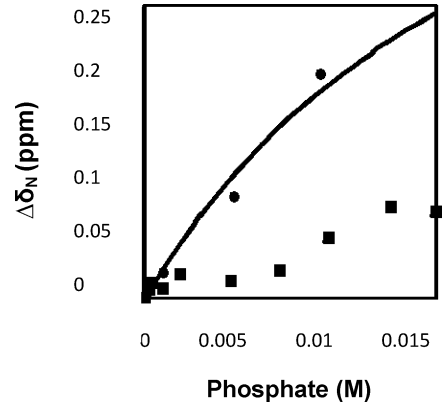

FIGURE 3: Comparison of IP_3 and phosphate binding to profilin. The binding curves illustrate the changes in profilin His 119 amide nitrogen chemical shifts upon binding to either IP_3 (●) or phosphate (■). The shifts are plotted on a per phosphate basis to allow for direct comparison.

the possibility that a fraction of the chemical shift perturbations is due not to a direct interaction but to a change in protein conformation upon IP_3 binding. Indeed, a modest helical increase has been observed previously upon profilin binding to PI(4,5)P_2 (*20*). To address this issue, we used an R88L profilin mutant, as this residue has been shown to be important for PI(4,5)P_2 binding in several independent studies (*26, 33, 35*). In this mutant, IP_3 binding is no longer observed at or near residue 88, suggesting that this subsite is rendered nonfunctional by this mutation. Instead, two widely separated regions (approximately 30 Å apart) experience chemical shift perturbations in the presence of IP_3: a region around R135/R136 and a second around K69/K90. These data provide strong evidence for a multivalent complex between profilin and PI(4,5)P_2 or IP_3 and suggest binding by at least three separate molecules. This stoichiometry

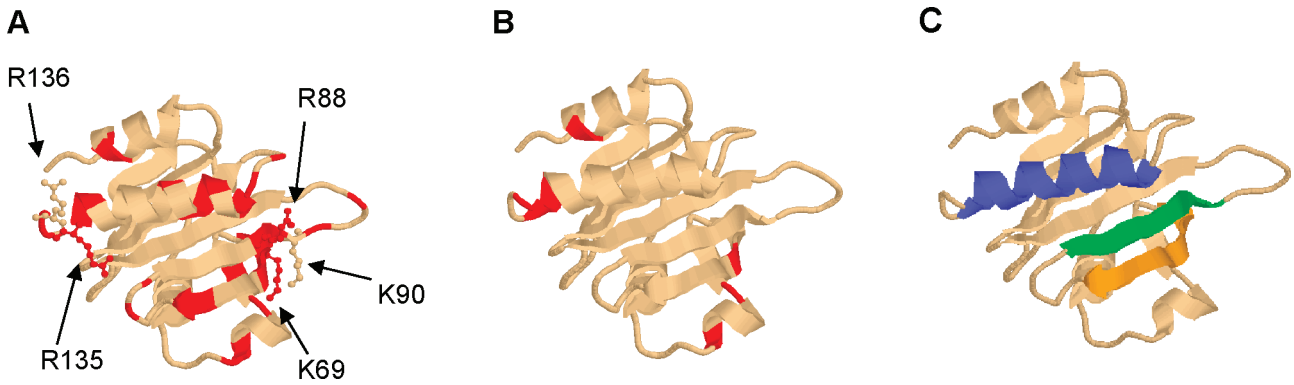

FIGURE 4: Comparison of IP_3 binding surfaces for wild-type and R88L profilin. Highlighted in red are the residues for which a chemical shift change was observed upon IP_3 binding. Shown in ball and stick representation are residues K69/K90, R88, and R135/R136. The structure in panel A shows shifts from the wild-type profilin experiment whereas that in panel B shows shifting residues that were derived from the R88L titration series. The structure in panel C shows residues from helix D (blue), β-strand D (orange), and β-strand E (green). The mutation of site R88 eliminates many of the residues that were affected by IP_3 binding, but binding is still evident around R135/R136 and to a lesser extent near K69/K90.

Table 2: Calculated K_d and $\Delta\delta_{max}$ Values for Each Shifting Residue of the R88L Mutant and the Error Associated with Each Value

residue	K_d (mM)	K_d error (mM)	$\Delta\delta_{max}$ (ppm)
Y6 ^{15}N	34.3	14.5	−0.39
S57 ^{15}N	14.3	5.4	−0.20
G62 ^{1}H	23.0	13.2	0.04
S71 ^{1}H	17.5	11.1	0.03
L134 ^{1}H	30.8	13.1	0.05
R135 ^{1}H	63.8	33.2	0.12
R136 ^{1}H	27.1	23.9	0.03
Y139 ^{1}H	65.3	115.4	0.09

agrees reasonably well with previous estimates for the profilin:$PI(4,5)P_2$ ratio of 1:5, as determined in lipid vesicles, and may suggest that such experiments overestimate the stoichiometric ratio (*39, 42*).

The data obtained with the R88L mutant also provide support for the role of K69/K90 in $PI(4,5)P_2$ binding. Previous mutation of these residues to glutamate results in only a 25−35% change in affinity (*34*). Nonetheless, the affinity of this subsite for IP_3 in the R88L mutant is indistinguishable from that in wild-type profilin, suggesting that the two subsites, although closely spaced, act independently. Similarly, modest changes in $PI(4,5)P_2$ affinity have been observed for the mutations R88A, R135D, and R135/R136A, though an R136D mutation leads to a more significant decrease in binding affinity (*33*). This situation is reminiscent of $PI(4,5)P_2$ binding by FERM domain proteins. These proteins contain three separate clusters of basic residues, approximately 20−40 Å apart. Mutation of a single cluster of basic residues has only a modest effect on the binding of ezrin to $PI(4,5)P_2$, whereas mutation of two or more clusters completely abrogates lipid binding (*60*). Importantly, only one of these sites is implicated in the cocrystal structure of the FERM protein radixin with IP_3, suggesting that crystallographic studies may fail to detect all biochemically important binding sites (*61*). In contrast, the use of IP_3 in our NMR titration appears to detect all three subsites in profilin.

In summary, we have established that IP_3 is an effective probe for studying the interaction between profilin and $PI(4,5)P_2$, in spite of the fact that profilin distinguishes between IP_3 and $PI(4,5)P_2$ under physiological conditions (*46*). Our data also clearly demonstrate that the $PI(4,5)P_2$ binding sites on the surface of profilin overlap with the binding sites of both actin and PLP, providing a structural basis for understanding the means by which profilin may be regulated by PIs (*29, 37*). Moreover, because multivalent interactions between cytoskeletal proteins and PIs are quite common, this method can easily be extended to study the regulation of other multivalent $PI(4,5)P_2$ binding proteins including FERM proteins, cofilin, gelsolin, vinculin, WASP-Scar, and α-actinin (*60, 62−69*).

At least ten structurally distinct PI-binding domains have been identified, and numerous other PI proteins have been identified that contain no canonical PI domain, complicating the study of protein•PI interactions (*11−14, 31, 39, 40, 64, 65, 70, 71*). In addition, $PI(4,5)P_2$ is only one of seven PIs with known physiological roles (*1*). It is likely that the appropriate soluble PI headgroup ligands can also be used to study the structural basis of PI regulation by lipids including PIP_3, $PI(3,4)P_2$, $PI(3,5)P_2$, and the three known PIP species. The small size of these soluble PI ligands makes them applicable not just for NMR studies but for a variety of assays from which the entire lipid structure would be excluded due to its particle size or the unpredictable aggregation properties.

ACKNOWLEDGMENT

The authors thank Travis Graham and Melissa Shaw for laboratory assistance.

REFERENCES

1. Di Paolo, G., and De Camilli, P. (2006) Phosphoinositides in cell regulation and membrane dynamics. *Nature 443*, 651–657.
2. McLaughlin, S., Wang, J., Gambhir, A., and Murray, D. (2002) PIP2 and proteins: interactions, organization, and information flow. *Annu. Rev. Biophys. Biomol. Struct. 31*, 151–175.
3. Vanhaesebroeck, B., Leevers, S. J., Ahmadi, K., Timms, J., Katso, R., Driscoll, P. C., Woscholski, R., Parker, P. J., and Waterfield, M. D. (2001) Synthesis and function of 3-phosphorylated inositol lipids. *Annu. Rev. Biochem. 70*, 535–602.
4. Downes, C. P., Gray, A., and Lucocq, J. M. (2005) Probing phosphoinositide functions in signaling and membrane trafficking. *Trends Cell Biol. 15*, 259–268.
5. Niggli, V. (2001) Structural properties of lipid-binding sites in cytoskeletal proteins. *Trends Biochem. Sci. 26*, 604–611.
6. Janmey, P. A., and Lindberg, U. (2004) Cytoskeletal regulation: rich in lipids. *Nat. Rev. Mol. Cell Biol. 5*, 658–666.

7. McLaughlin, S., and Murray, D. (2005) Plasma membrane phosphoinositide organization by protein electrostatics. *Nature 438*, 605–611.
8. De Matteis, M. A., and Godi, A. (2004) PI-loting membrane traffic. *Nat. Cell Biol. 6*, 487–492.
9. Haucke, V. (2005) Phosphoinositide regulation of clathrin-mediated endocytosis. *Biochem. Soc. Trans. 33*, 1285–1289.
10. Golebiewska, U., Gambhir, A., Hangyas-Mihalyne, G., Zaitseva, I., Radler, J., and McLaughlin, S. (2006) Membrane-bound basic peptides sequester multivalent (PIP2), but not monovalent (PS), acidic lipids. *Biophys. J. 91*, 588–599.
11. Balla, T. (2005) Inositol-lipid binding motifs: signal integrators through protein-lipid and protein-protein interactions. *J. Cell Sci. 118*, 2093–2104.
12. Hurley, J. H. (2006) Membrane binding domains. *Biochim. Biophys. Acta 1761*, 805–811.
13. Lemmon, M. A. (2003) Phosphoinositide binding domains. *Traffic 4*, 201–213.
14. Cho, W., and Stahelin, R. V. (2005) Membrane-protein interactions in cell signaling and membrane trafficking. *Annu. Rev. Biophys. Biomol. Struct. 34*, 119–151.
15. Machesky, L. M., and Pollard, T. D. (1993) Profilin as a potential mediator of membrane cytoskeleton communication. *Trends Cell Biol. 3*, 381–385.
16. Papayannopoulos, V., Co, C., Prehoda, K. E., Snapper, S., Taunton, J., and Lim, W. A. (2005) A polybasic motif allows N-WASP to act as a sensor of PIP2 density. *Mol. Cell 17*, 181–191.
17. Yin, H. L., and Janmey, P. A. (2003) Phosphoinositide regulation of the actin cytoskeleton. *Annu. Rev. Physiol. 65*, 761–789.
18. Witke, W. (2004) The role of profilin complexes in cell motility and other cellular processes. *Trends Cell Biol. 14*, 461–469.
19. Jockusch, B. M., Murk, K., and Rothkegel, M. (2007) The profile of profilins. *Rev. Physiol., Biochem., Pharmacol. 159*, 131–149.
20. Lu, P. J., Shieh, W. R., Rhee, S. G., Yin, H. L., and Chen, C. S. (1996) Lipid products of phosphoinositide 3-kinase bind human profilin with high affinity. *Biochemistry 35*, 14027–14033.
21. Pollard, T. D. (2007) Regulation of actin filament assembly by Arp2/3 complex and formins. *Annu. Rev. Biophys. Biomol. Struct. 36*, 451–477.
22. Witke, W., Sutherland, J. D., Sharpe, A., Arai, M., and Kwiatkowski, D. J. (2001) Profilin I is essential for cell survival and cell division in early mouse development. *Proc. Natl. Acad. Sci. U.S.A. 98*, 3832–3836.
23. Lambrechts, A., Jonckheere, V., Peleman, C., Polet, D., De Vos, W., Vandekerckhove, J., and Ampe, C. (2006) Profilin-I-ligand interactions influence various aspects of neuronal differentiation. *J. Cell Sci. 119*, 1570–1578.
24. Roy, P., and Jacobson, K. (2004) Overexpression of profilin reduces the migration of invasive breast cancer cells. *Cell Motil. Cytoskeleton 57*, 84–95.
25. Janke, J., Schluter, K., Jandrig, B., Theile, M., Kolble, K., Arnold, W., Grinstein, E., Schwartz, A., Estevez-Schwarz, L., Schlag, P. M., Jockusch, B. M., and Scherneck, S. (2000) Suppression of tumorigenicity in breast cancer cells by the microfilament protein profilin 1. *J. Exp. Med. 191*, 1675–1685.
26. Wittenmayer, N., Jandrig, B., Rothkegel, M., Schlueter, K., Arnold, W., Haensch, W., Scherneck, S., and Jockusch, B. M. (2004) Tumor suppressor activity of profilin requires a functional actin binding site. *Mol. Biol. Cell 15*, 1600–1608.
27. Feldner, J. C., and Brandt, B. H. (2002) Cancer cell motility-on the road from c-erbB-2 receptor steered signaling to actin reorganization. *Exp. Cell Res. 272*, 93–108.
28. Wu, N., Zhang, W., Yang, Y., Liang, Y.-L., Wang, L.-Y., Jin, J.-W., Cai, X.-M., and Zha, X.-L. (2006) Profilin 1 obtained by proteomic analysis in all-trans retinoic acid-treated hepatocarcinoma cell lines is involved in inhibition of cell proliferation and migration. *Proteomics 6*, 6095–6106.
29. Schutt, C. E., Myslik, J. C., Rozycki, M. D., Goonesekere, N. C. W., and Lindberg, U. (1993) The structure of crystalline profilin-b-actin. *Nature 365*, 810–816.
30. Bjoerkegren, C., Rozycki, M., Schutt, C. E., Lindberg, U., and Karlsson, R. (1993) Mutagenesis of human profilin locates its poly(L-proline)-binding site to a hydrophobic patch of aromatic amino acids. *FEBS Lett. 333*, 123–126.
31. Lassing, I., and Lindberg, U. (1985) Specific interaction between phsophatidylinositol 4,5-bisphosphate and profilactin. *Nature 314*, 835–838.
32. Goldschmidt-Clermont, P. J., Machesky, L. M., Doberstein, S. K., and Pollard, T. D. (1991) Mechanism of the interaction of human platelet profilin with actin. *J. Biol. Chem. 113*, 1081–1089.
33. Lambrechts, A., Jonckheere, V., Dewitte, D., Vandekerckhove, J., and Ampe, C. (2002) Mutational analysis of human profilin I reveals a second PI(4,5)-P_2 binding site neighbouring the poly-(L-proline) binding site. *BMC Biochem. 3*, 12.
34. Skare, P., and Karlsson, R. (2002) Evidence for two interaction regions for phosphatidylinositol(4,5)-bisphosphate on mammalian profilin I. *FEBS Lett. 522*, 119–124.
35. Sohn, R. H., Chen, J., Koblan, K. S., Bray, P. F., and Goldschmidt-Clermont, P. J. (1995) Localization of a binding site for phosphatidylinositol 4,5-bisphosphate on human profilin. *J. Biol. Chem. 270*, 21114–21120.
36. Chaudhary, A., Chen, J., Gu, Q.-M., Witke, W., Kwiatkowski, D. J., and Prestwich, G. D. (1998) Probing the phosphoinositide 4,5-bisphosphate binding site of human profilin I. *Chem. Biol. 5*, 273–281.
37. Mahoney, N. M., Janmey, P. A., and Almo, S. C. (1997) Structure of the profilin-poly-L-proline complex involved in morphogenesis and cytoskeletal regulation. *Nat. Stuct. Biol. 4*, 953–960.
38. Schaaf, G., Ortlund, E. A., Tyeryar, K. R., Mousley, C. J., Ile, K. E., Garrett, T. A., Ren, J., Woolls, M. J., Raetz, C. R. H., Redinbo, M. R., and Bankaitis, V. A. (2008) Functional anatomy of phospholipid binding and regulation of phosphoinositide homeostasis by proteins of the Sec14 superfamily. *Mol. Cell 29*, 191–206.
39. Goldschmidt-Clermont, P. J., Machesky, L. M., Baldassare, J. J., and Pollard, T. D. (1990) The actin-binding protein profilin binds to PIP2 and inhibits its hydrolysis by phospholipase C. *Science 247*, 1575–1578.
40. Lemmon, M. A. (2008) Membrane recognition by phospholipid-binding domains. *Nat. Rev. Mol. Cell Biol. 9*, 99–111.
41. Itoh, T., Koshiba, S., Kigawa, T., Kikuchi, A., Yokoyama, S., and Takenawa, T. (2001) Role of the ENTH domain in phosphatidylinositol-4,5-bisphosphate binding and endocytosis. *Science 291*, 1047–1051.
42. Machesky, L. M., Goldschmidt-Clermont, P. J., and Pollard, T. D. (1990) The affinities of human platelet and Acanthamoeba profilin isoforms for polyphosphoinositides account for their relative abilities to inhibit phospholipase C. *Cell Regul. 1*, 937–950.
43. Lassing, I., and Lindberg, U. (1988) Specificity of the interaction between phosphatidylinositol 4,5-bisphosphate and the profilin: actin complex. *J. Cell. Biochem. 37*, 255–267.
44. Tuominen, E. K., Holopainen, J. M., Chen, J., Prestwich, G. D., Bachiller, P. R., Kinnunen, P. K., and Janmey, P. A. (1999) Fluorescent phosphoinositide derivatives reveal specific binding of gelsolin and other actin regulatory proteins to mixed lipid bilayers. *Eur. J. Biochem. 263*, 85–92.
45. Ostrander, D. B., Gorman, J. A., and Carman, G. M. (1995) Regulation of profilin localization in Saccharomyces cerevisiae by phosphoinositide metabolism. *J. Biol. Chem. 270*, 27045–27050.
46. Goldschmidt-Clermont, P. J., Kim, J. W., Machesky, L. M., Rhee, S. G., and Pollard, T. D. (1991) Regulation of phospholipase C-gamma 1 by profilin and tyrosine phosphorylation. *Science 251*, 1231–1233.
47. Czech, M. P. (2003) Dynamics of phosphoinositidesin membrane retrieval and insertion. *Annu. Rev. Physiol. 65*, 791–815.
48. Moens, P. D. J., and Bagatolli, L. A. (2007) Profilin binding to sub-micellar concentrations of phosphatidylinositol (4,5) bisphosphate and phosphatidylinositol (3,4,5) trisphosphate. *Biochim. Biophys. Acta 1768*, 439–449.
49. Studier, F. W., Rosenberg, A. H., Dunn, J. J., and Dubendorff, J. W. (1990) Use of T7 RNA polymerase to direct expression of cloned genes. *Methods Enzymol. 185*, 60–89.
50. Almo, S. C., Pollard, T. D., Way, M., and Lattman, E. E. (1994) Purification, characterization and crystallization of Acanthamoeba profilin expressed in Escherichia coli. *J. Mol. Biol. 236*, 950–952.
51. Fedorov, A. A., Pollard, T. D., and Almo, S. C. (1994) Purification, characterization and crystallization of human platelet profilin expressed in Escherichia coli. *J. Mol. Biol. 241*, 480–482.
52. Edelhoch, H. (1967) Spectroscopic determination of tryptophan and tyrosine in proteins. *Biochemistry 6*, 1948–1954.
53. Metzler, W. J., Constantine, K. L., Friedrichs, M. S., Bell, A. J., Ernst, E. G., Lavoie, T. B., and Mueller, L. (1993) Characterization of the three-dimensional solution structure of human

profilin: proton, carbon-13, and nitrogen-15 NMR assignments and global folding pattern. *Biochemistry 32*, 13818–13829.

54. Czerwinski, R. M., Johnson, W. H., Jr., Whitman, C. P., Harris, T. K., Abeygunawardana, C., and Mildvan, A. S. (1997) Kinetic and structural effects of mutations of the catalytic amino-terminal proline in 4-oxalocrotonate tautomerase. *Biochemistry 36*, 14551–14560.
55. Ye, J., Kohli, L. L., and Stone, M. J. (2000) Characterization of binding between the chemokine eotaxin and peptides derived from the chemokine receptor CCR3. *J. Biol. Chem. 275*, 27250–27257.
56. Metzler, W. J., Farmer, B. T., II, Constantine, K. L., Friedrichs, M. S., Lavoie, T., and Mueller, L. (1995) Refined solution structure of human profilin I. *Protein Sci. 4*, 450–459.
57. Mammen, M., Seok-Ki, C., and Whitesides, G. M. (1998) Polyvalent interactions in biological systems: Implications for design and use of multivalent ligands and inhibitors. *Angew. Chem., Int. Ed. Engl. 37*, 2754–2794.
58. Kiessling, L. L., Gestwicki, J. E., and Strong, L. E. (2006) Synthetic multivalent ligands as probes of signal transduction. *Angew. Chem., Int. Ed. Engl. 45*, 2348–2368.
59. Lundquist, J. J., and Toone, E. J. (2002) The cluster glycosidic effect. *Chem. Rev. 102*, 555–578.
60. Barret, C., Roy, C., Montcourrier, P., Mangeat, P., and Niggli, V. (2000) Mutagenesis of the phosphatidylinositol 4,5-bisphosphate (PIP(2)) binding site in the NH(2)-terminal domain of ezrin correlates with its altered cellular distribution. *J. Cell Biol. 151*, 1067–1080.
61. Hamada, K., Shimizu, T., Matsui, T., Tsukita, S., and Hakoshima, T. (2000) Structural basis of the membrane-targeting and unmasking mechanisms of the radixin FERM domain. *EMBO J. 19*, 4449–4462.
62. Moriyama, K., Yonezawa, N., Sakai, H., Yahara, I., and Nishida, E. (1992) Mutational analysis of an actin-binding site of cofilin and characterization of chimeric proteins between cofilin and destrin. *J. Biol. Chem. 267*, 7240–7244.
63. Ojala, P. J., Paavilainen, V., and Lappalainen, P. (2001) Identification of yeast cofilin residues specific for actin monomer and PIP2 binding. *Biochemistry 40*, 15562–15569.
64. Yu, F. X., Sun, H. Q., Janmey, P., and Yin, H. L. (1992) Identification of a polyphosphoinositide binding sequence in an actin monomer-binding domain of gelsolin. *J. Biol. Chem. 267*, 14616–14621.
65. Feng, L., Mejillano, M., Yin, H. L., Chen, J., and Prestwich, G. D. (2001) Full-contact domain labeling: identification of a novel phosphoinositide binding site on gelsolin that requires the complete protein. *Biochemistry 40*, 904–913.
66. Yin, H. L., Iida, K., and Janmey, P. A. (1988) Identification of a polyphosphoinositide-modulated domain in gelsolin which binds to the sides of actin filaments. *J. Cell Biol. 106*, 805–812.
67. Ziegler, W. H., Liddington, R. C., and Critchley, D. R. (2006) The structure and regulation of vinculin. *Trends Cell Biol. 16*, 453–460.
68. Prehoda, K. E., Scott, J. A., Mullins, R. D., and Lim, W. A. (2000) Integration of multiple signals through cooperative regulation of the N-WASP-Arp2/3 complex. *Science 290*, 801–806.
69. Fukami, K., Furuhashi, K., Inagaki, M., Endo, T., Hatano, S., and Takenawa, T. (1992) Requirement of phosphatidylinositol 4,5-bisphosphate for α-actinin function. *Nature 359*, 150–152.
70. Wang, J., Gambhir, A., Hangyas-Mihalyne, G., Murray, D., Golbebiewska, U., and McLaughlin, S. (2002) Lateral sequestration of phosphatidylinositol 4,5-bisphospate by the basic effector domain of myristolated alanine-rich C kinase substrate is due to nonspecific electrostatic interaction. *J. Biol. Chem. 277*, 34401–34412.
71. Lorenz, C. D., Faraudo, J., and Travesset, A. (2008) Hydrogen bonding and binding of polybasic residues with negatively charged mixed lipid monolayers. *Langmuir 24*, 1654–1658.

BI801535F